PV- and Warm Conveyor Belt Analysis of a North Atlantic Cyclone

Christopher Rausch
ETH Zürich / University of Bonn (Rheinische Friedrich-Wilhelms-Universität Bonn)

1 Main questions & conclusion

- **Q:** Of what kind and how strong is the influence of the PV anomaly in the WCB outflow? **A:** The outflow anomaly induces a wind field that leads to a north advection of the cyclone (see box 2).
- **Q:** How does the spatial evolution of the WCB look like? **A:** The WCB shows a dichotomous structure, where the two airstreams differ in their ascend regions (see box 3).
- **Q:** How do the traced variables evolve along the two different branches? **A:** Statistically anticyclonic turning WCB trajectories start with higher θ and q and ascend faster and higher than cyclonic ones (see box 4).

2 Piecewise PV- Inversion (PPVI)

- In order to quantify the influence of the negative PV anomaly in the WCB outflow, a piecewise PV inversion is performed.
- The cyclogenesis event of this case study starts on the 31.12.2015 06 UTC.
- Trajectories are used to spatially isolate the WCB outflow and its PV anomaly.

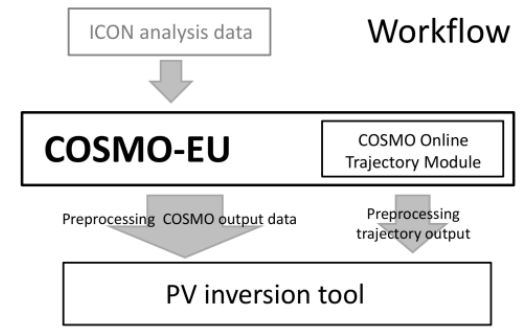

- Outcome: The induced wind field of the PV anomaly in the WCB outflow leads to a north advection of the upper tropospheric PV structure above the cyclone with rates of ± 0.2 PVU/h and hence supports the north advection of the cyclone.
- The figure below shows the attributed disturbances of the outflow anomaly in the wind- and geopotential field gained with the piecewise PV inversion.

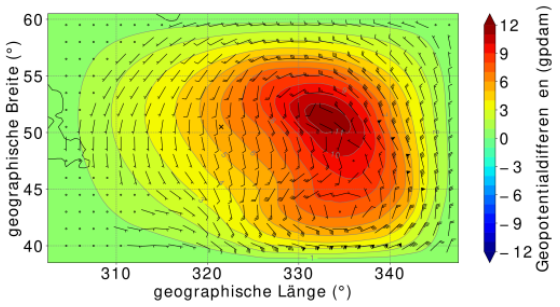

Fig 2. 300hPa: Attributed disturbances of the WCB outflow anomaly at t=45 in geopotential ϕ (colour, gpdam) and horizontal wind $v_{h,p}$ (arrows, km/h), x-axis: longitude, y-axis: latitude.

3 WCB analysis: dichotomous structure

- WCB trajectory filter criterion (Joos et al 2012):
  $max(\Delta p)_{\Delta t \leq 48\,h} > 600\,\mathrm{hPa}$
- Similar to Martinez-Alvarado et al (2013) the WCB shows a dichotomous structure (fig. 2).
- The cyclonic branch forms 24 hours after the anticyclonic branch.
- Anticyclonic WCB trajectories start ahead of the cold front and more south west. Their percentage on the trajectory number decreases with time (fig 3).
- Cyclonic WCB trajectories start behind the warm front and more close to the cyclone center. Their percentage increases with time.

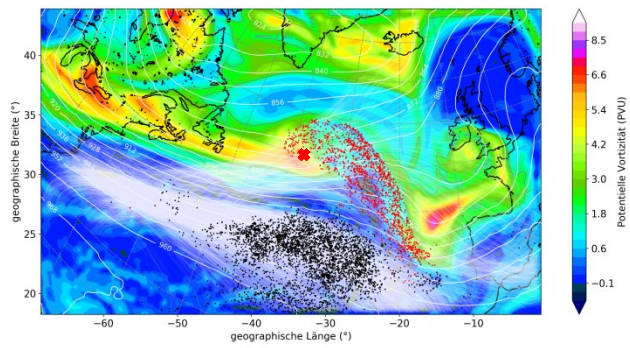

Fig. 2. forecast hour 45: 300 hPa PV distribution (colour), horizontal positions of those WCB trajectories (10th part) of the anticyclonic (black dots) and the cyclonic branch (red dots) that reached the upper troposphere (p<400hPa) together with their total trajectories (white) and cyclone position (red cross).

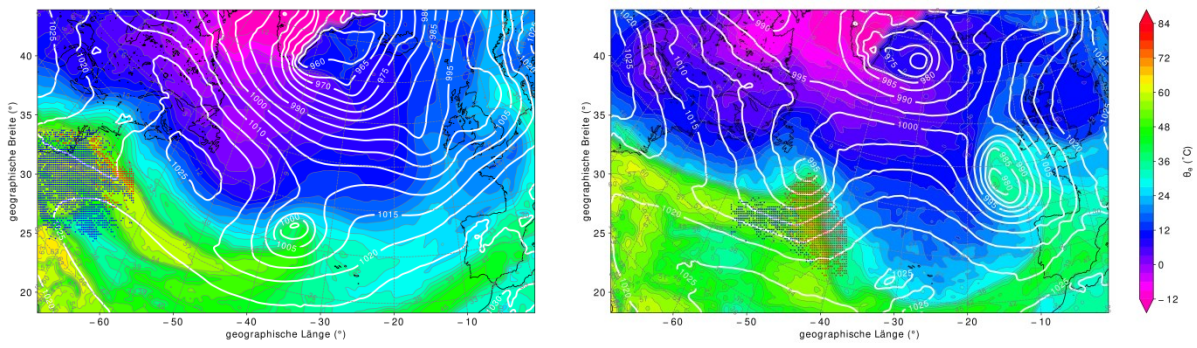

Fig. 3. Starting positions (5th part) of the WCB trajectories of the anticyclonic (blue) and the cyclonic branch (red) started at forecast hour 0 (left picture) / 30 (right picture) fulfilling the ascent criterion until forecast hour 48/66, pseudo potential temperature θ_e (°C, colour) and MSLP (hPa, white contours).

4 WCB analysis: traced variables

- The WCB trajectories of the two branches were pretty well separable using θ_{max} = 319 K as a threshold.
- Trajectories of the anticyclonic branch start with higher values of q and θ than trajectories of the cyclonic branch.
- Anticyclonic trajectories release more latent heat during ascent (due to their higher q), therefore ascend faster and reach higher maximum values of PV than cyclonic ones.
- Cyclonic trajectories move far more north during their ascend.

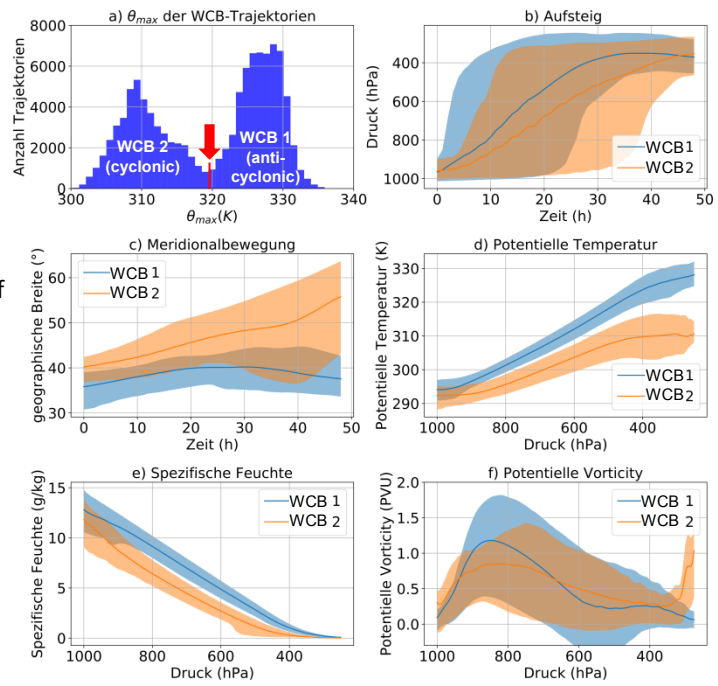

Fig. 4. a) histogram for the maximum potential temperature along the trajectories, y-axis denotes the trajectory number for each column; b) ascend (hPa, y-axis) vs time (h, x-axis); c) meridional position (°, y-axis) vs time (h, x-axis); d)-f) potential temperature (K) / specific humidity (g/kg) / PV (PVU) vs pressure (hPa, y-axis).
Blue: anticyclonic branch, orange: cyclonic branch.
Bold lines denote the mean value, shaded areas denote the 5th and 95th percentiles, in case of the potential vorticity 25th and 75th percentiles have been used.

5 References

– Davis, Christopher A, 1992: *Piecewise potential vorticity inversion*. Journal of the Atmospheric Sciences 49.16, 1397–1411.
– Joos, H., and H. Wernli, 2012: *Influence of microphysical processes on the potential vorticity development in a warm conveyor belt: A case-study with the limited-area model COSMO*. Quart. J. Roy. Meteor. Soc., 138, 407–418.
– Langguth, M., 2016: *Analyse von zyklogenetischen Prozessen unter Verwendung von PV-Inversionstechniken*. Rheinische Friedrich-Wilhelms-Universität Bonn
– Martínez-Alvarado, O., H. Joos, J. Chagnon, M. Boettcher, S. L. Gray, R. S. Plant, J. Methven, and H. Wernli, 2014: *The dichotomous structure of the warm conveyor belt*. Quart. J. Roy. Meteor. Soc., 140, 1809–1824.
– Miltenberger, A.K., S. Pfahl and H. Wernli, 2013: *An online trajectory module (version 1.0) for the nonhydrostatic numerical weather prediction model COSMO*. Geosci. Model Dev., Vol.6, Issue 6.
– Wernli, H. and H. C. Davies, 1997: *A Lagrangian-based analysis of extratropical cyclones. I: The method and some applications*. Quart. J. Roy. Meteor. Soc., 123, 467–489.

From the master thesis of Christopher Rausch 2019
PV- und Warm-Conveyor-Belt-Analyse einer nordatlantischen Zyklone. Rheinische Friedrich-Wilhelms-Universität Bonn